Physics of the Dark Universe 37 (2022) 101116

Contents lists available at ScienceDirect

Physics of the Dark Universe

journal homepage: www.elsevier.com/locate/dark

Scalar induced gravitational waves from warm inflation

Richa Arya [a,*], Arvind Kumar Mishra [b]

[a] Department of Physics, Indian Institute of Science, Bangalore, 560002, India
[b] Indian Institute of Science Education and Research, Pune, 411008, India

ARTICLE INFO

Article history:
Received 4 August 2022
Accepted 12 September 2022

Keywords:
Warm inflation
Primordial black holes
Scalar induced gravitational waves

ABSTRACT

Stochastic gravitational waves can be induced from the primordial curvature perturbations generated during inflation, through scalar–tensor mode coupling at the second order of cosmological perturbation theory. Here we discuss a model of warm inflation in which large curvature perturbations are generated at the small scales because of inflaton dissipation. These overdense perturbations then collapse at later epoch to form primordial black holes, as was studied in our earlier work (Ref. Arya (2020)), and therefore may also act as a source to the second-order tensor perturbations. In this study, we calculate the spectrum of these secondary gravitational waves from our warm inflationary model. We find that our model leads to a generation of scalar induced gravitational waves (SIGW) over a frequency range $\sim (1\text{–}10^6)$ Hz. Further, we discuss the detection possibilities of these SIGWs, taking in account the sensitivity of different ongoing and future gravitational wave experiments.

1. Introduction

The inflationary paradigm of the early Universe is a widely known phase of a rapid accelerated expansion, which resolves many issues of the Standard Model of cosmology [1–5]. Additionally, it also generates density perturbations for all the structures we see today. During inflation, the primordial (scalar, vector, tensor) perturbations of a vast range of wavelengths are generated. According to the decomposition theorem, at the linear order of cosmological perturbation theory, these perturbation modes evolve independently. The scalar fluctuations are imprinted as the temperature anisotropies in the Cosmic Microwave Background (CMB) radiation and further become the seed density perturbations that grow into large-scale structures (LSS) at the late time. On the large scales 10^{-4} Mpc$^{-1} < k < 1$ Mpc^{-1}, the amplitude of the primordial scalar curvature perturbations has been precisely measured to a value $\Delta^2_{\mathcal{R}}(k_P) = 2.1 \times 10^{-9}$ [6]. The tensor perturbations signature on the CMB as B-mode polarization have not been detected till date. However an upper limit has been imposed on the amplitude of the primordial tensor fluctuations, through the observable tensor-to-scalar ratio r. The latest observations of BICEP/Keck have put a constraint on $r < 0.036$ at 95% confidence level [7]. A detection of primordial gravitational waves would provide information about the energy scale of inflation and thus is important to understand the physics of early Universe. For a review on inflationary cosmology, see Refs. [8–12].

Besides the linear theory, the scalar perturbations can also couple to the tensor perturbations and generate secondary gravitational waves at the second order of cosmological perturbation theory [13–15]. These SIGWs are inevitably associated with the primordial black hole (PBH) production from different inflationary models and are used to constraint the abundance of PBHs [16–22]. Primordial Black Holes [23–26], i.e. black holes with a primordial origin, serve as a probe to a huge range of small scales, unexplored by the CMB and LSS observations. They can form in a number of ways — by the collapse of overdense fluctuations [24,25], from the collision of bubbles [27], by the collapse of strings [28,29] or domain walls [30], etc. As for PBH generation, the amplitude of the primordial curvature power spectrum at small scales is hugely amplified $\mathcal{O}(10^{-2})$, it is quite evident that these large scalar perturbations then act as a source term to the second-order tensor fluctuations. In literature, the generation of primordial black holes and the associated secondary gravitational waves has been investigated for many inflationary models, for example, running mass inflation [31,32], double inflation [33], axion curvaton model [34], hybrid inflation with chaotic potentials [35], inflation with gravitationally enhanced friction [36], chaotic inflation [37], models with noncanonical kinetic term [38, 39], Gauss–Bonnet-corrected single field inflation [40], inflection point models [41], ultraslow roll and punctuated inflation [42], k and G inflation [43], etc. The spectrum of these scalar induced gravitational waves (SIGW) can be constrained through various ongoing and future gravitational wave experiments [44–46], such as Pulsar Timing Array (PTA [47], NANOGrav [48], and SKA [49]), second-generation GW interferometers (advanced LIGO, VIRGO, KAGRA [50]), space based GW interferometers (LISA [51], DECIGO, BBO [52]), third-generation GW interferometers (Einstein

* Corresponding author.
E-mail addresses: richaarya@iisc.ac.in (R. Arya), arvind.mishra@acads.iiserpune.ac.in (A.K. Mishra).

https://doi.org/10.1016/j.dark.2022.101116
2212-6864/

Telescope (ET) [53], Cosmic Explorer (CE) [54]). For a review, see Refs. [55,56].

In this study, we consider a scenario, known as *warm inflation* [57–59], in which the dynamics of the Universe is governed by the dissipative and non-equilibrium effects in a coupled inflaton–radiation system. In this description, the inflaton interactions to the other fields are not neglected during inflation, unlike in the standard cold inflation, and there is a non-zero temperature in the Universe throughout the inflationary phase. The background evolution as well as the perturbations of the inflaton field are modified due to its coupling with other fields. As a result, the primordial power spectrum and thus the predicted observables in warm inflation differ from those in cold inflation. (For a review, see Refs. [60,61].) Warm inflation is well-motivated for multiple reasons, as will be discussed in Section 2. In the literature, many warm inflationary models are constrained in the context of CMB observations [62–67], however the small scale features of warm inflation are not well explored. Recently, we had studied the formation of primordial black holes during radiation dominated era, in a model of warm inflation [68]. We found that for some parameter space, we can successfully explain the CMB on large scales as well as generate light mass PBHs (nearly 10^3 g) of a significant abundance. More recently, the authors of Ref. [69] carried out a study on the secondary gravity waves and PBH production in a scalar warm little inflaton model. They found that PBHs with mass lighter than 10^6 g and a spectrum of GW peaked at $\sim(10^5 - 10^6)$ Hz could be generated in their model.

In this work, we aim to discuss the secondary gravitational waves induced by the large scalar curvature perturbations in warm inflation. To this extent, we consider a quartic potential ($V(\phi) = \lambda\phi^4$) and a dissipation coefficient cubicly dependent on temperature ($\Upsilon \propto T^3$). The motivation of considering this potential is that it is the simplest single-field warm inflation model which, for some parameter space, is consistent with the CMB observations and also predicts a large amplitude of scalar power spectrum on the very small scales, leading to PBH formation. Further, as the second order tensor modes are coupled with the first order scalar modes, we expect a spectrum of secondary gravitational wave induced by the large scalar fluctuations. Indeed, we find that our warm inflationary model leads to a GW spectrum with a significant amplitude over the frequency range $\sim (1 - 10^6)$ Hz, which may be explored in the future high frequency detectors, such as the levitated-sensor detector [70], microwave cavities [71], decameter Michelson interferometers [72], resonant mass detectors [73]. We will discuss it in detail in Section 4.

This paper is organized as follows: In Section 2, we discuss the basics of warm inflation theory, the background evolution of inflaton, dissipation coefficient and the primordial curvature power spectrum of warm inflation. Then in Section 3, we discuss the spectrum of induced gravitational waves sourced by the scalar curvature perturbations. After this, we discuss our model of warm inflation and the results obtained in Section 4 and then finally summarize the paper in Section 5. We also present an Appendix for the calculation of dissipation coefficient in warm inflation.

2. Warm Inflation

Warm Inflation is a description of inflation in which one considers dissipative processes during the inflationary phase. In contrast to the standard cold inflation, where one neglects the inflaton couplings to other fields during the slow-roll inflationary phase, warm inflation is a more general and natural description, where the inflaton interactions to other fields are considered. In this picture, the inflaton dissipates its energy into radiation fields, and as a result of which there is a non-zero temperature in the Universe during the inflationary phase. Depending on the strength of inflaton dissipation, warm inflation is classified into two dissipative regimes — weak and strong, characterized by a dissipation parameter Q defined as the ratio of the inflaton dissipation rate to the Hubble expansion rate.

Warm inflation is motivated for multiple reasons: At first, it is a more complete picture of inflation and has cold inflation as its limiting case. As particle production takes place simultaneously with the expansion during warm inflation, a separate reheating phase may not be required in some models [74]. Warm inflation predicts unique and distinct characteristics from cold inflation on the CMB. For certain inflationary models, which are ruled out from Planck observations, the tensor-to-scalar ratio predictions are lowered in the warm inflation description, and thus they are viable models for some range of dissipation [63–67]. Besides the Gaussian two-point correlations, warm inflation can also lead to non-Gaussianities because of the inflaton interactions and hence can be tested in the future CMB experiments [75,76]. In warm inflation, the conditions for slow roll are modified due to an extra friction term in the inflaton equation of motion. Thus, warm inflation is less restrictive in the flatness of the potential, and thus may relax the η problem [77]. Warm inflation models, like in Refs. [78–81] might also provide a unified explanation for inflation, dark matter and/or dark energy, and thus interesting to explore. Also, warm quintessential inflation model can generate a unique spectrum of high frequency primordial gravitational waves, which could be tested in future GW missions [82]. It has been found that some models of warm inflation can also explain the baryon-asymmetry of the Universe [83,84].

Further, warm inflation predicts interesting signatures at the small scales. In Ref. [68], we found that the primordial power spectrum is blue-tilted ($n_s > 1$) on the small scales, and has a large amplitude, which leads to the formation of primordial black holes. This feature of warm inflation was further explored and the spectrum of scalar induced gravitational waves associated with PBH production was analysed in Ref. [69]. Furthermore, as inflation is a low energy effective field theory, it has to obey some criteria, such as the swampland distance and de-Sitter conjectures, in order to embed it in a UV complete theory. It has been found that single-field slow roll cold inflation, with a canonical kinetic term and a Bunch Davies vacuum, is not in accordance with the swampland conjectures. However, recent studies show that warm inflation models with a large value of the dissipation parameter [85,86] can satisfy the swampland conjectures, thus making it in agreement with a high energy theory. All these above features arise from the fundamental feature of treating the dynamics of inflaton as that of a dissipative system, and hence makes warm inflation interesting. Thus, a comprehensive study of the warm inflation scenario is necessary to understand the physics of the early Universe.

2.1. Background evolution equations

In the warm inflation description, one considers the dissipative processes during inflation based on the principles of non-equilibrium field theory for interacting quantum fields [87,88]. The inflaton is assumed to be near-equilibrium and evolving slowly as compared to the microphysics timescales in the adiabatic approximation. The effective equation of motion of inflaton field is obtained using the Schwinger–Keldysh close time path formalism of thermal field theory. (For a review, see Refs. [89,90]). Due to its couplings, the equation of motion is modified by an additional friction term $\Upsilon\dot{\phi}(t)$ and is given by [88,91]

$$\ddot{\phi}(t) + 3H\dot{\phi}(t) + \Upsilon\dot{\phi}(t) + V'(\phi) = 0. \tag{1}$$

Here a dot ($\dot{}$) and a prime ($'$) represents derivative of the quantity w.r.t time and field ϕ, respectively. The dissipation coefficient

$\Upsilon(\phi, T)$ depends on the mechanism of inflaton dissipation, such as the channel of decay, the coupling strengths, and the multiplicities of the fields involved. We define a dissipation parameter $Q = \Upsilon/3H$ and rewrite Eq. (1) as

$$\ddot{\phi}(t) + 3H(1+Q)\dot{\phi}(t) + V'(\phi) = 0. \tag{2}$$

When the dissipation parameter is smaller than the Hubble expansion rate ($Q < 1$), it is the weak dissipative regime, and when it is larger ($Q > 1$), then it is the strong dissipative regime of warm inflation.

From the continuity equation, we can also write the energy density of the inflaton ρ_ϕ and radiation ρ_r as,

$$\dot{\rho_\phi} + 3H(p_\phi + \rho_\phi) = -\Upsilon\dot{\phi}^2. \tag{3}$$

$$\dot{\rho}_r + 4H\rho_r = \Upsilon\dot{\phi}^2\ . \tag{4}$$

The negative sign on the right-hand side of Eq. (3) shows that the inflaton dissipates its energy with time. As a result of the dissipation, radiation is produced along with the expansion during warm inflation, as can be seen on Eq. (4). Assuming that the radiation thermalizes quickly after being produced, we have $\rho_r = \frac{\pi^2}{30} g_* T^4$ where T is the temperature of the thermal bath, g_* is the number of relativistic degrees of freedom present during warm inflation.

2.1.1. Slow roll parameters and conditions

The flatness of the potential $V(\phi)$ in inflation is measured in terms of the potential slow roll parameters, similar to the ones defined for cold inflation

$$\epsilon_\phi = \frac{M_{Pl}^2}{16\pi}\left(\frac{V'}{V}\right)^2, \qquad \eta_\phi = \frac{M_{Pl}^2}{8\pi}\left(\frac{V''}{V}\right). \tag{5}$$

In addition to these, in warm inflation there are other slow roll parameters defined as [92,93]

$$\beta_\Upsilon = \frac{M_{Pl}^2}{8\pi}\left(\frac{\Upsilon' V'}{\Upsilon V}\right), \qquad b = \frac{TV'_{,T}}{V'}\ , \qquad c = \frac{T\Upsilon_{,T}}{\Upsilon}. \tag{6}$$

Here the subscript $_{,T}$ represents derivative of the quantity w.r.t T. These additional slow roll parameters are a measure of the field and temperature dependence in the inflaton potential and the dissipation coefficient. The stability analysis of warm inflationary solution shows that the following conditions should be satisfied during the slow roll [93]

$$\epsilon_\phi \ll 1+Q, \qquad |\eta_\phi| \ll 1+Q, \qquad |\beta_\Upsilon| \ll 1+Q,$$
$$0 < b \ll \frac{Q}{1+Q}, \qquad |c| < 4. \tag{7}$$

As can be clearly seen, for large Q, these conditions relax the requirement for the potential to be extremely flat, as the upper limit on the slow roll parameters ϵ_ϕ, η_ϕ is increased. Therefore, the η problem is not as severe in warm inflation.

2.1.2. Evolution equations in the slow roll approximation

In the slow roll approximation, we can neglect $\ddot{\phi}$ in Eq. (2) which gives

$$\dot{\phi} \approx \frac{-V'(\phi)}{3H(1+Q)}, \tag{8}$$

and since $\dot{\rho}_r$ is smaller than the other terms in Eq. (4) throughout inflation, we can approximate $\dot{\rho}_r \approx 0$ and obtain

$$\rho_r \approx \frac{\Upsilon}{4H}\dot{\phi}^2 = \frac{3}{4}Q\dot{\phi}^2. \tag{9}$$

2.2. Dissipation coefficient

The microphysics of the coupled inflaton–radiation system results into a dissipation coefficient in the inflaton equation of motion. Depending on the interaction Lagrangian, the channel of inflaton decay, the coupling strengths, and the multiplicities of the fields involved, there are different model constructions of warm inflation. In the earlier ones, it was realized that it is difficult to obtain a successful strong dissipative regime, as the thermal corrections to the effective potential are large [91,94]. Therefore, subsequent studies considered models, such as the supersymmetric distributed mass model in the context of string theory [59,95], or a two-stage decay mechanism of inflaton, where the inflaton couples to a heavy intermediate catalyst field which then further couple to the light radiation fields [96,97] or recently discrete interchange symmetry in the warm little inflaton model [98,99] to control these corrections, and attain a strong dissipation regime of warm inflation. Here we will consider a two-stage decay of the inflaton in a supersymmetric inflation model [100,101]. In this, we have three superfields Φ, X, and Y, whose scalar and fermion components are (ϕ, ψ_ϕ), (χ, ψ_χ) and (σ, ψ_σ), respectively. The interacting superpotential is given as

$$W = g\Phi X^2 + hXY^2, \tag{10}$$

where g and h are the coupling strengths between $\Phi - X$, and $X - Y$, respectively. The scalar inflaton is coupled with the intermediate bosonic and fermionic components of the X superfield (also called catalyst fields), which subsequently decay into the scalar and fermionic components of the Y superfield (called radiation fields). The radiation fields are considered to be lighter than the catalyst fields. The scatterings of decay products σ, ψ_σ with masses $m_\sigma, m_{\psi_\sigma} \ll T$ is sufficient to keep them thermalized and constitute the thermal bath, as shown in the Appendix C of Ref. [102]. The inflaton particle states are also assumed to thermalize with a same temperature, for some range of effective couplings [102]. The scalar part of the Lagrangian is given as

$$\begin{aligned} -\mathcal{L}_s &= |\partial_\Phi W|^2 + |\partial_X W|^2 + |\partial_Y W|^2 \\ &= g^2|\chi|^4 + h^2|\sigma|^4 + 4g^2|\chi|^2|\phi|^2 \\ &\quad + 4ghRe[\phi^\dagger\chi^\dagger\sigma^2] + 4h^2|\chi|^2|\sigma|^2. \end{aligned} \tag{11}$$

The scalar fields ϕ, χ, σ are chosen to be complex, $\chi = (\chi_1 + i\chi_2)/\sqrt{2}$, and similarly for others. When the background scalar field ϕ takes an expectation value $\varphi/\sqrt{2}$, the mass of the χ field is given as: $m_{\chi_1} = \sqrt{2}g\varphi$, $m_{\chi_2} = \sqrt{2}g\varphi$. The Yukawa interactions are obtained as

$$-\mathcal{L}_Y = \frac{1}{2}\sum_{n,m}\frac{\partial^2 W}{\partial\zeta_n\,\partial\zeta_m}\bar{\psi}_n P_L\psi_m + \frac{1}{2}\sum_{n,m}\frac{\partial^2 W^\dagger}{\partial\zeta_n^\dagger\,\partial\zeta_m^\dagger}\bar{\psi}_n P_R\psi_m \tag{12}$$

where ζ refers to the superfields Φ, X, Y and $P_L = 1 - P_R = (1+\gamma_5)/2$. For the superpotential given in Eq. (10), the Yukawa interactions are given as

$$-\mathcal{L}_Y = g\phi\bar{\psi}_\chi P_L\psi_\chi + 2g\chi\bar{\psi}_\phi P_L\psi_\chi + h\chi\bar{\psi}_\sigma P_L\psi_\sigma + 2h\sigma\bar{\psi}_\chi P_L\psi_\sigma + h.c. \tag{13}$$

For these interaction terms, the dissipation coefficient is calculated, as shown in Appendix. In this study, we choose the special case, when the intermediate catalyst fields are heavy, which gives $\Upsilon = C_\phi T^3/\phi^2$ in the low temperature limit.

2.3. Primordial curvature power spectrum

In warm inflation description, as there is a temperature in the Universe throughout the inflationary phase, therefore the

fluctuations in the inflaton field are also sourced by the thermal noise, unlike in the cold inflation where the inflaton has only quantum fluctuations. The total primordial curvature power spectrum for warm inflation by including both quantum and thermal contributions to the inflaton power spectrum is given as [64,92,98,103–106]

$$\Delta^2_{\mathcal{R}}(k) = \left(\frac{H_k^2}{2\pi\dot{\phi}_k}\right)^2 \left[\, 1 + 2n_k + \left(\frac{T_k}{H_k}\right) \frac{2\sqrt{3}\pi Q_k}{\sqrt{3+4\pi Q_k}} \,\right] G(Q_k). \tag{14}$$

Here is the description of each term present in this equation:

- The prefactor $\left(\frac{H_k^2}{2\pi\dot{\phi}_k}\right)^2$ is the primordial curvature power spectrum in the cold inflation. It shows that in the limit $Q \to 0$ and $T \to 0$, we recover the standard cold inflation from warm inflation.
- Due to the presence of the radiation bath in warm inflation, the inflaton can also be excited from its vacuum state to Bose–Einstein distribution, given as $n_k = \frac{1}{\exp(\frac{k/a_k}{T_k})-1}$. The system of inflaton particles and radiation fields is assumed to thermalize with a same temperature, and the scattering rates are shown in Ref. [102].
- Due to the thermal noise contributions to the inflaton fluctuations, the primordial power spectrum has terms dependent on the dissipation coefficient and the temperature of the thermal bath, as given by the third term in the square bracket.
- The perturbations in the radiation can also couple to the inflaton perturbations and lead to a growth in the primordial power spectrum [103]. This growth factor $G(Q_k)$ depends on the form of dissipation coefficient and is obtained numerically [64,98]. For the form of dissipation coefficient under consideration $\Upsilon \propto T^3$,

$$G(Q_k) = 1 + 4.981\, Q_k^{1.946} + 0.127\, Q_k^{4.330}. \tag{15}$$

  In the weak dissipation regime, the growth factor does not enhance the power spectrum significantly. But in the strong dissipation regime, the power spectrum is considerably enhanced due to the growth factor.

Further, it is interesting to note that in the strong dissipation regime, the shear effects in radiation also become important which cause damping of the power spectrum [104], and therefore the overall growth in the power spectrum is reduced. In the expression for the primordial power spectrum given above, we do not account for any shear effects.

3. Scalar induced gravitational waves spectrum

In this Section, we briefly review the gravitational waves spectrum induced from the scalar perturbations at second order of cosmological perturbation theory. For a more detailed derivation, we suggest Refs. [14,15,107,108]. To start with, we consider a perturbed metric in the longitudinal gauge with vanishing vector perturbations as

$$ds^2 = -a^2\,(1+2\Phi)\,d\eta^2 + a^2\left[(1-2\Psi)\,\delta_{ij} + \frac{h_{ij}}{2}\right] dx^i dx^j \tag{16}$$

where a is the scale factor and η is the conformal time. Here Φ, Ψ are the scalar and h_{ij} correspond to the tensor metric perturbations, respectively. In our notation, the spatial coordinates i, j, k, etc. can take values 1, 2, 3. In this work, we focus our analysis for vanishing anisotropic stress for which $\Phi = \Psi$. However, in Ref. [15], it has been found that effect of anisotropic stress, i.e., $\Phi \neq \Psi$, is very small.

The second order action for graviton can be given as

$$S = \frac{M_{\rm Pl}^2}{32} \int d^3x\, d\eta\, a^2 \left(h'_{ij}h'_{ij} - h_{ij,k}h_{ij,k}\right) \tag{17}$$

where $M_{\rm Pl} = 1/\sqrt{8\pi G}$ is the reduced Planck mass, $h_{ij,k}$ represents derivative of h_{ij} w.r.t. spatial coordinate and in this Section a prime represents the differentiation of any quantity w.r.t. conformal time η. We do a Fourier decomposition of tensor $h_{ij}(\eta, \mathbf{x})$ as

$$h_{ij}(\eta, \mathbf{x}) = \int \frac{d^3\mathrm{k}}{(2\pi)^{\frac{3}{2}}} \left[e^{+}_{ij}(\mathbf{k}) h^{+}_{\mathbf{k}}(\eta) + e^{\times}_{ij}(\mathbf{k}) h^{\times}_{\mathbf{k}}(\eta)\right] e^{i\mathbf{k}\cdot\mathbf{x}} \tag{18}$$

where $e^{+}_{ij}(\mathbf{k})$ and $e^{\times}_{ij}(\mathbf{k})$ are time independent, traceless, transverse vectors. These quantities are defined in terms of orthonormal basis, $e_i(\mathbf{k})$, $\bar{e}_i(\mathbf{k})$ as

$$e^{+}_{ij}(\mathbf{k}) = \frac{1}{\sqrt{2}}\left[e_i(\mathbf{k})e_j(\mathbf{k}) - \bar{e}_i(\mathbf{k})\bar{e}_j(\mathbf{k})\right] \tag{19}$$

$$\text{and} \quad e^{\times}_{ij}(\mathbf{k}) = \frac{1}{\sqrt{2}}\left[e_i(\mathbf{k})\bar{e}_j(\mathbf{k}) + \bar{e}_i(\mathbf{k})e_j(\mathbf{k})\right]. \tag{20}$$

Further, the power spectrum of tensor perturbation is defined as

$$\langle h^{\lambda}_{\mathbf{k}}(\eta) h^{\lambda'}_{\mathbf{k}'}(\eta)\rangle = \frac{2\pi^2}{k^3}\delta_{\lambda\lambda'}\delta^3(\mathbf{k}+\mathbf{k}')\mathcal{P}_h(\eta, k) \tag{21}$$

where, $\lambda, \lambda' = +, \times$ corresponds to the polarization index and $\mathcal{P}_h(\eta, k)$ is the dimensionless tensor power spectrum. In our calculation, we assume parity invariance, which provides the same result for both the polarizations.

To obtain $P_h(\eta, k)$, we first need to explore the dynamics of tensor mode, which can be obtained by using the Einstein's equation. The evolution of tensor mode sourced by the scalar perturbation is given as [108]

$$h''_{\mathbf{k}}(\eta) + 2\mathcal{H}h'_{\mathbf{k}}(\eta) + \mathrm{k}^2 h_{\mathbf{k}}(\eta) = 4S_{\mathbf{k}}(\eta) \tag{22}$$

where $\mathcal{H}$ is the conformal Hubble parameter, and $S_{\mathbf{k}}(\eta)$ is the source term with quadratic contributions from scalar perturbations given by

$$S_{\mathbf{k}}(\eta) = \int \frac{d^3q}{(2\pi)^{\frac{3}{2}}} e_{ij}(\mathbf{k}) q_i q_j \left[2\Phi_{\mathbf{q}}\Phi_{\mathbf{k}-\mathbf{q}} + \frac{4}{3(1+w)}\left(\mathcal{H}^{-1}\Phi'_{\mathbf{q}} + \Phi_{\mathbf{q}}\right)\left(\mathcal{H}^{-1}\Phi'_{\mathbf{k}-\mathbf{q}} + \Phi_{\mathbf{k}-\mathbf{q}}\right)\right]. \tag{23}$$

Further, to estimate $\langle h^{\lambda}_{\mathbf{k}}(\eta) h^{\lambda'}_{\mathbf{k}'}(\eta)\rangle$, one needs to evaluate $\langle S_{\mathbf{k}}(\eta) S_{\mathbf{k}'}(\eta')\rangle$, which in turn requires the dynamics of potential field Φ. The evolution of Φ is calculated using the Einstein's equation and is given as [108]

$$\Phi''_{\mathbf{k}} + 3\mathcal{H}(1+c_s^2)\Phi'_{\mathbf{k}} + \left[2\mathcal{H}' + (1+3c_s^2)\mathcal{H}^2 + c_s^2\mathrm{k}^2\right]\Phi_{\mathbf{k}} = \frac{a^2}{2}\tau\delta S$$

where $c_s^2 = \left(\frac{\delta p}{\delta\rho}\right)_S$ is the square of the speed of sound and δS is the entropy perturbation. The pressure and energy density perturbation are related as $\delta P = c_s^2\delta\rho + \tau\delta S$. To simplify the analysis, we assume that $\delta S = 0$ and sound speed is constant, $c_s^2 = w$. Further, we parameterize the scalar field as $\Phi_{\mathbf{k}} = \Phi(\mathrm{k}\eta)\phi_{\mathbf{k}}$, where $\phi_{\mathbf{k}}$ is its primordial fluctuation and $\Phi(\mathrm{k}\eta)$ correspond to the transfer function. The two point correlation function for primordial fluctuation is given as

$$\langle \phi_{\mathbf{k}}\phi_{\mathbf{k}'}\rangle = \frac{2\pi^2}{k^3}\delta^3(\mathbf{k}+\mathbf{k}')\left(\frac{3+3w}{5+3w}\right)^2 \mathcal{P}_\zeta(\mathrm{k}) \tag{24}$$

where $\mathcal{P}_\zeta(\mathrm{k})$ is the primordial curvature perturbations. Equipped with this expression, we will next obtain $\mathcal{P}_h(\eta, k)$.

The solution for $h_{\mathbf{k}}(\eta)$ can be obtained by applying the Green's function method in Eq. (22) as

$$h_{\mathbf{k}}(\eta) = \frac{4}{a(\eta)} \int d\tilde{\eta}\; G_{\mathbf{k}}(\eta, \tilde{\eta})\; a(\tilde{\eta})\; S_{\mathbf{k}}(\tilde{\eta}) \tag{25}$$

where $G_{\mathbf{k}}(\eta, \tilde{\eta})$ is the solution of differential equation

$$G''_{\mathbf{k}}(\eta, \tilde{\eta}) + \left[\mathrm{k}^2 - \frac{a''(\eta)}{a(\eta)}\right] G_{\mathbf{k}}(\eta, \tilde{\eta}) = \delta(\eta - \tilde{\eta}). \tag{26}$$

Then, using Eqs. (21) and (25), we get[1] [15]

$$\begin{aligned}\langle h_{\mathbf{k}}(\eta) h_{\mathbf{k}'}(\eta')\rangle =& \frac{16}{a^2(\eta)} \int_{\eta_0}^{\eta} d\tilde{\eta}_2 \int_{\eta_0}^{\eta} d\tilde{\eta}_1\; a(\tilde{\eta}_1) a(\tilde{\eta}_2) \\ &\times\; G_{\mathbf{k}}(\eta, \tilde{\eta}_1) G_{\mathbf{k}'}(\eta, \tilde{\eta}_2) \langle S_{\mathbf{k}}(\eta) S_{\mathbf{k}'}(\eta')\rangle. \end{aligned} \tag{27}$$

Morever, to estimate the correlation function, $\langle S_{\mathbf{k}}(\eta) S_{\mathbf{k}'}(\eta')\rangle$, we do not consider non-Gaussianity in the primordial curvature power spectrum. With this assumption, we equate Eq. (21) with Eq. (27) and after some simplification obtain [15,108]

$$\begin{aligned}\mathcal{P}_h(\eta, k) =& 4 \int_0^\infty dv \int_{|1-v|}^{|1+v|} du \left[\frac{4v^2 - (1 + v^2 - u^2)^2}{4vu}\right]^2 \\ &\times\; \mathrm{I}^2(v, u, x) P_\zeta(kv) P_\zeta(ku) \end{aligned} \tag{28}$$

where, $u = |\mathbf{k} - \tilde{\mathbf{k}}|/\mathrm{k}$ and $v = \tilde{\mathrm{k}}/\mathrm{k}$ are the dimensionless variable in which $\tilde{\mathrm{k}}$ corresponds for the wave vector associated with the scalar source $\Phi_{\tilde{\mathbf{k}}}$. In this expression, $x \equiv k\eta$ and the function $\mathrm{I}(v, u, x)$ is given as

$$\mathrm{I}(v, u, x) = \int_0^x d\tilde{x}\; \frac{a(\tilde{\eta})}{a(\eta)}\; \mathrm{k}\; G_{\mathbf{k}}(\eta, \tilde{\eta})\, f(v, u, \tilde{x}). \tag{29}$$

The function $f(v, u, \tilde{x})$ consists of Φ terms and is given in Ref. [108]. Further, after redefining the variable $s = u - v$ and $t = u + v - 1$, we may rewrite the Eq. (28) as

$$\begin{aligned}\mathcal{P}_h(\eta, k) =& 2 \int_0^\infty dt \int_{-1}^{1} ds \left[\frac{t(t+2)(s^2-1)}{(1+t+s)(1+t-s)}\right]^2 \\ &\times\; \mathrm{I}^2(v, u, x) P_\zeta(kv) P_\zeta(ku). \end{aligned} \tag{30}$$

The gravitational wave energy density defined as $\rho_{\mathrm{GW}}(\eta) = \int d\ln \mathrm{k}\; \rho_{\mathrm{GW}}(\eta, \mathrm{k})$ can be estimated for the subhorizon modes as [109]

$$\rho_{\mathrm{GW}} = \frac{\mathrm{M}_{pl}^2}{16a^2} \overline{\langle h_{ij,k}\; h_{ij,k}\rangle} \tag{31}$$

where the overline correspond to the oscillation average. The fraction of gravitational wave energy density per logarithmic k interval to the total energy is given by

$$\begin{aligned}\Omega_{\mathrm{GW}}(\eta, k) =& \frac{1}{\rho_{\mathrm{tot}}(\eta)} \left(\frac{d\rho_{\mathrm{GW}}(\eta)}{d\ln \mathrm{k}}\right) = \frac{\rho_{\mathrm{GW}}(\eta, \mathrm{k})}{\rho_{\mathrm{tot}}(\eta)} \\ =& \frac{1}{24} \left(\frac{\mathrm{k}}{a(\eta)H(\eta)}\right)^2 \overline{P_h(\eta, \mathrm{k})} \end{aligned} \tag{32}$$

where $\rho_{\mathrm{tot}}(\eta)$ is the total energy density and $\overline{P_h(\eta, \mathrm{k})}$ is the dimensionless power spectrum averaged over time, estimated using Eq. (30). In this calculation, we have summed over both the polarization modes. For a radiation dominated Universe, in the late time limit, $x \to \infty$, the function $\overline{\mathrm{I}^2(v, u, x)}$ can be simplified as [108]

$$\begin{aligned}\overline{\mathrm{I}^2(v, u, x \to \infty)} =& \frac{9}{2x^2} \left(\frac{u^2 + v^2 - 3}{4u^3 v^3}\right)^2 \times \\ & \left[\left(-3uv + (u^2 + v^2 - 3) \log\left|\frac{3 - (u+v)^2}{3 - (u-v)^2}\right|\right)^2 \right. \\ & \left. + \pi^2 (u^2 + v^2 - 3)^2 \theta(u + v - \sqrt{3})\right]. \end{aligned} \tag{33}$$

Substituting Eq. (33) in Eq. (30) and carrying out the integral for $\mathcal{P}_h(\eta, k)$, we finally obtain $\Omega_{\mathrm{GW}}(\eta, k)$ from Eq. (32).

The observationally relevant quantity is the energy spectrum of induced gravitational waves $\Omega_{GW,0}(k)$ at the present time given by

$$\Omega_{\mathrm{GW},0}(k) = 0.39 \left(\frac{g_\star(T_c)}{106.75}\right)^{-\frac{1}{3}} \Omega_{r,0}\; \Omega_{\mathrm{GW}}(\eta_c, k) \tag{34}$$

where $\Omega_{r,0}h^2 = 4.18 \times 10^{-5}$ is the present radiation energy density, and $g_\star(T_c)$ is the effective number of relativistic degree of freedom in the radiation dominated era. Also, η_c is the conformal time at the epoch when perturbation is inside the horizon after re-entry during radiation dominated era. Morever, the frequency of gravitational wave is related with the comoving scale as

$$f = \frac{k}{2\pi} = 1.5 \times 10^{-15} \left(\frac{k}{1\ \mathrm{Mpc}^{-1}}\right) \mathrm{Hz}. \tag{35}$$

Using this relation, we express $\Omega_{\mathrm{GW},0(k)}$ in terms of frequency of the gravitational wave.

4. Analysis and discussion

We consider a monomial potential ($V(\phi) = \lambda\phi^4$) of warm inflation with the dissipation coefficient $\Upsilon = C_\phi T^3/\phi^2$. Monomial potentials of inflation are single parameter models and are interesting as they predict a large value of primordial gravitational waves, which leads to their testability in future CMB experiments. In our earlier work [65], we had considered this model and estimated the parameter space of model variables consistent with the CMB observations. We found that unlike cold inflation, where $\lambda\phi^4$ potential is ruled out, there is a parameter space in warm inflation for which this potential can be a viable model for describing inflation. Also, the predicted value of the tensor-to-scalar ratio in this model can be tested in the future CMB polarization experiments. Next, in another work [68], we found that interestingly this warm inflation model has features with a blue-tilted spectrum and a large amplitude of the primordial power spectrum at the small scales. This leads to the formation of PBHs with mass $M_{PBH} \sim 10^3$ g. Further, we found that some parameter space of our warm inflation model is consistent with the bounds on the PBH mass fraction and thus interesting to explore. Furthermore, we expect that associated with the enhanced scalar power spectrum, there would be second order tensor modes. To complete the picture, we now extend our previous studies and explore the secondary induced gravitational waves from our warm inflation model.

4.1. Primordial curvature power spectrum

We first show the evolution of dissipation parameter as a function of number of efolds of inflation and the growth factor $G(Q_k)$ in Fig. 1. Here the number of efolds are counted from the end of inflation ($N_e = 0$) such that the pivot scale corresponds to $N_P = 60$. In this model of warm inflation, we have [65]

$$\frac{dQ}{dN} = -40 \left(\frac{9(\pi^2 g_*/30)^3}{64 C_\phi^4 \lambda}\right)^{\frac{1}{5}} \frac{Q^{6/5}(1+Q)^{6/5}}{(1+7Q)}. \tag{36}$$

[1] In the r.h.s. of this obtained equation, there is a discrepancy of a factor of 16 in Ref. [15] and Ref. [108]. This is because the source term in the evolution equation of $h_{\mathbf{k}}$ in Eq. (22) are differently defined in the two references.

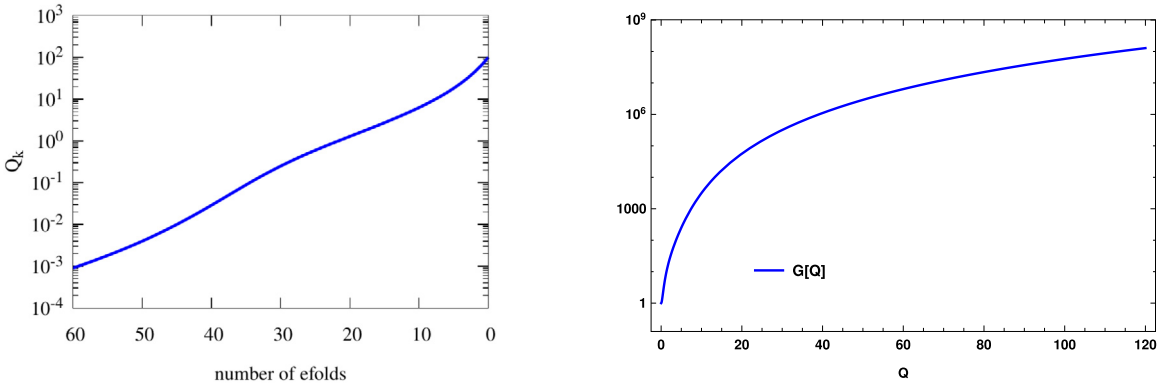

Fig. 1. *Left:* The evolution of dissipation parameter Q_k versus number of efolds of inflation for our warm inflation model and *Right:* the growth factor $G(Q)$ versus Q, given in Eq. (15) are shown here.

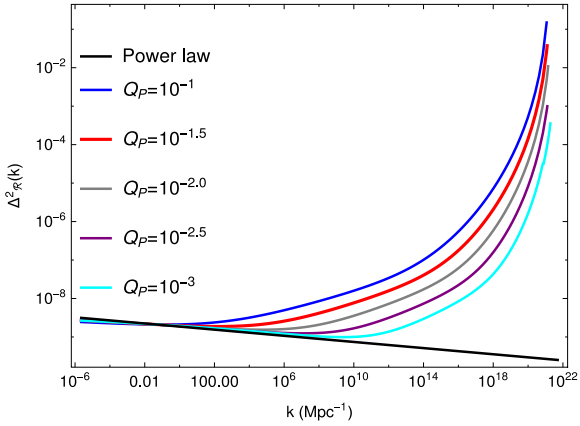

Fig. 2. The primordial curvature power spectrum for different values of dissipation parameter Q_P as a function of the scale k.
Source: Figure taken from Ref. [68]

The negative sign of dQ/dN implies that the dissipation parameter Q increases as the inflation proceeds such that it evolves from weak dissipative regime at the pivot scale to a strong dissipative regime near the end of inflation, as can be seen in Fig. 1. As the growth function is proportional to the dissipation parameter through Eq. (15), there is a huge enhancement in the $G(Q)$ (Fig. 1) and subsequently the primordial power spectrum near the end of inflation, as shown in Fig. 2.

We can see from Fig. 2 that the primordial power spectrum is red-tilted ($n_s < 1$) for the CMB scales and for some range of Q_P values, it is consistent with the $n_s - r$ bounds from Planck observations. Along with, it has features that it is blue-tilted ($n_s > 1$) at the small scales with a large amplitude, due to a large growth factor. The enhanced amplitude of scalar fluctuations at small scales then source the formation of primordial black holes and furthermore secondary gravitational waves.

4.2. Spectral index and tensor-to-scalar ratio

In Fig. 3, we plot the scalar spectral index, defined as the tilt of primordial power spectrum at the pivot scale,

$$n_s - 1 \equiv \left.\frac{d\ln\Delta^2_{\mathcal{R}}(k)}{d\ln k}\right|_{k=k_P}. \tag{37}$$

We see that only weak dissipative regime can be consistent with the n_s values in this model. In the same Figure, we also plot the tensor-to-scalar ratio, defined as the ratio of the amplitude of the tensor power spectrum to the amplitude of the scalar power spectrum at the pivot scale

$$r \equiv \frac{\Delta^2_t(k_P)}{\Delta^2_{\mathcal{R}}(k_P)}. \tag{38}$$

We can see that the value of r decreases as the dissipation parameter increases.

We find that for parameter space $[6.31 \times 10^{-4} < Q_P < 0.02]$, our warm inflation model is consistent with the observationally allowed $n_s - r$ values. Therefore, we will explore the small scale features of our warm inflation model for this range of Q_P values.

4.3. Induced gravitational wave spectrum

Using Eqs. (30), (32), and (34), we calculate the induced gravitational wave spectrum for the primordial power spectrum of warm inflation given in Eq. (14). Then using Eq. (35), we plot the present spectral energy density of the produced secondary gravitational waves as a function of the frequency in Fig. 4. We also include the theoretical constraints on $\Omega_{GW,0}$ and sensitivity curves for the present and future gravitational wave detectors in the figure. For details, see Ref. [44–46,109–111] and references therein. Here is a summary of various constraints on the spectral energy density and sensitivities of different gravitational wave detectors.

Constraints on the primordial gravitational wave background

- **Big-Bang Nucleosynthesis (BBN)**: The presence of large amplitude of gravitational waves at the time of BBN, alters the light nuclei abundances predicted by the standard BBN. This gives a constraint on the GW background as, $\Omega_{\rm GW,0} < 1.5 \times 10^{-5}$ corresponding to frequency $\nu > 10^{-10}$ Hz today [109,112].
- **Cosmic Microwave Background (CMB):** The presence of extra relativistic degrees of freedom or large energy density of GW at the time of recombination may change the epoch of matter-radiation equality and acoustic oscillations [113]. This gives an upper bound on the GW background as $\Omega_{\rm GW,0} < 2.7 \times 10^{-6}$ corresponding to frequencies $\nu > 10^{-15}$ Hz [114,115].
- **Second generation GW detectors — LIGO/VIRGO** [50]**:** The bounds on energy density of the gravitational waves from direct ground based detectors are $\Omega_{\rm GW,0} < 6.9 \times 10^{-6}$ through LIGO S5 run with a maximum sensitivity at frequency $\sim$ 100 Hz [44], $\Omega_{\rm GW,0} < 10^{-9}$ in Advanced LIGO/VIRGO at frequency $\nu \sim 30$ Hz [116], $\Omega_{\rm GW,0} < 10^{-10}$ in LIGO++ [117].

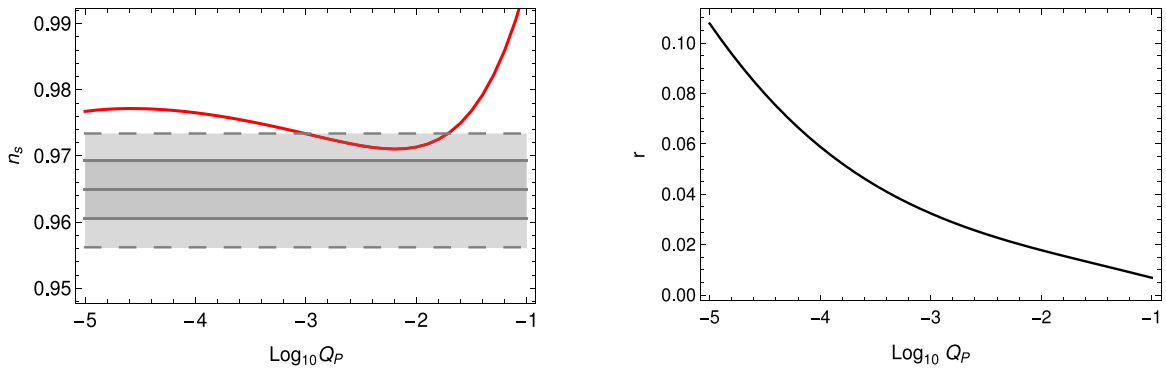

Fig. 3. *Left:* The spectral index or tilt of the primordial curvature power spectrum for our warm inflation model. The colored band represents the allowed $1-2\sigma$ range of n_s from the Planck observations. Here the number of efolds of inflation equals to 60. *Right:* Tensor-to-scalar ratio as a function of Q_P is plotted here.

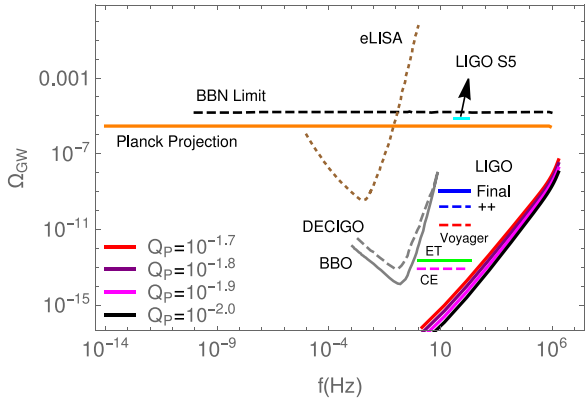

Fig. 4. The spectrum of secondary gravitational waves Ω_{GW} at the present time, generated for our warm inflation model as a function of the frequency of gravitational wave. (For interpretation of the references to color in this figure legend, the reader is referred to the web version of this article.)
Source: The sensitivity plots of various detectors are taken from Ref. [111] and references therein.

- **Space-based GW detectors — LISA [51], BBO, DECIGO [52]:** LISA is a planned space GW detector, which is expected to detect primordial gravitational wave background to $\Omega_{\mathrm{GW},0} < 10^{-10}$ at $\nu \sim 1$ mHz [118,119]. BBO [120] and DECIGO [121] are also future projects with proposed ability to detect GW down to $\Omega_{\mathrm{GW},0} \approx 10^{-16}$ at frequency $\nu \sim 1$ Hz.
- **Pulsar Timing Array (PTA) Experiments [47]:** Pulsars can be used as very stable clocks. These objects emit radio signals as pulses. By measuring the time of arrival of the radio pulses on Earth, one can detect perturbations due to gravitational waves. For $\nu \sim 10^{-8}$ Hz, the bound on GW energy density is $\Omega_{\mathrm{GW},0} < 4 \times 10^{-8}$ [122].
- **Third generation ground-based GW detectors — Einstein Telescope [53] Cosmic Explorer [54]:** ET is a proposed project with three detectors in triangle geometry, similar to LISA, whereas CE is a L-shaped geometry similar to advanced LIGO. The ET puts a limit on GW energy density $\Omega_{\mathrm{GW},0} < 4 \times 10^{-13}$ and from CE the bound is $\Omega_{\mathrm{GW},0} < 1.6 \times 10^{-13}$.

In Fig. 4, the solid colored lines (red, blue, magenta, black) correspond to various values of the parameter Q_P for our warm inflation model ($Q_P = 10^{-1.7}, 10^{-1.8}, 10^{-1.9}, 10^{-2.0}$, respectively). For these Q_P values, our model simultaneously explain the large scale CMB observations, as well as leads to the generation of PBHs and SIGW at the small scales. From the figure, it is evident that for stronger dissipation (large Q_P), the strength of the gravitational waves Ω_{GW} is large. Also, it is important to note that a majority of contribution to the primordial gravitational wave spectrum in Eq. (30) comes from the modes exiting the horizon near the end of inflation. These small scale modes with a large amplitude induce significant secondary gravitational waves over a frequency range $f = (1 - 10^6)$ Hz. This behavior can also be confirmed from Eq. (35).

Further, from the sensitivity curves of various observatories plotted in Fig. 4, we infer that the scalar induced gravitation waves produced from our model is quite feeble to be detected withing the current and near future interferometer GW detectors, operational for frequencies typically less than $\sim$ 10 kHz. However, with the new detection techniques designed for comparably larger frequency range, such as levitated-sensor-based gravitational-wave detector [70], microwave cavities [71], decameter Michelson interferometers [72], resonant mass detectors [73] (also see Refs. [123,124] for a comprehensive review), one hopes to scrutinize these models more efficiently and better understand the rich physics of the early Universe.

5. Summary

The inflationary paradigm of early universe uniquely predicts a spectrum of primordial gravitational waves. These have not been detected yet, however are important to understand the inflationary physics. Likewise, the small scale spectrum of primordial perturbations is not well measured and therefore an important aspect to explore the inflationary dynamics. Primordial black holes are one such remarkable probe of the small scales, that provide constrains on the primordial curvature power spectrum, and thus different inflationary models. As the amplitude of primordial curvature power spectrum is enhanced by many orders of magnitude for the formation of PBHs, there are also associated second-order tensor fluctuations sourced by the scalar fluctuations. The focus of this paper is to study these scalar induced gravitational waves from a model of warm inflation.

Warm Inflation is a well-motivated and general description of inflation where the dissipative and non-equilibrium processes are present during the inflationary phase. In this scenario, the inflaton dissipates into radiation fields during inflation, which modifies both the background inflaton dynamics as well as its perturbations. The primordial power spectrum of warm inflation is sourced dominantly by the thermal fluctuations, and thus has different predictions of observables than the cold inflation. Here we discuss a model of warm inflation with a quartic potential and a dissipation coefficient $\Upsilon \propto T^3$. In this model, we find that the dissipation parameter increases from weak dissipative regime at the pivot scale ($Q < 1$) to strong dissipative regime near the end of inflation ($Q \gg 1$). Accordingly, the growth factor in the primordial power spectrum $G(Q)$, characterizing the backreaction

of radiation fluctuations to the inflaton fluctuations, also increase tremendously. Thus, for certain parameter space of this model, there is a huge growth in the scalar curvature power spectrum on very small scales, leading to the formation of primordial black holes, as well as secondary gravitational waves.

We find that the strength of these secondary gravitational waves is directly proportional to the dissipation parameter, i.e. a large amplitude of present GW energy density implies a stronger dissipation, and vice-versa. Also, the modes exiting the horizon near the end of inflation with a large amplitude contribute majorly to the GW energy density. This corresponds to a GW spectrum over the frequency range $1 - 10^6$ Hz in our model. It is found that the generated spectrum does not lie in the sensitivities of different ongoing and future laser interferometer GW detectors. However, some more sensitive GW detectors, such as the levitated-sensor detector, microwave cavities, decameter Michelson interferometers, resonant mass detectors, will explore the high frequency spectrum of our proposed model and might test the feasibility of warm inflation model in future.

CRediT authorship contribution statement

Richa Arya: Conceptualization, Design, Analysis, Interpretation, Writing – original draft, Writing – review & editing. **Arvind Kumar Mishra:** Conceptualization, Design, Analysis, Interpretation, Writing – original draft, Writing – review & editing.

Declaration of competing interest

The authors declare that they have no known competing financial interests or personal relationships that could have appeared to influence the work reported in this paper.

Acknowledgments

We would like to acknowledge Prof. Raghavan Rangarajan, Prof. Namit Mahajan, and Prof. Rajeev Jain for useful discussions and suggestions. We also acknowledge the hospitality at Physical Research Laboratory, Ahmedabad during the initial stage of this work. Work of RA is supported by the National Post-Doctoral Fellowship by SERB, Government of India (PDF/2021/004792). AKM acknowledges the support through Ramanujan Fellowship (PI: Dr. Diptimoy Ghosh) offered by the Department of Science and Technology, Government of India (SB/S2/RJN-088/2018). All authors approved version of the manuscript to be published.

Appendix. Calculation of dissipation coefficient for our warm inflation model

Here we follow the lecture notes [125] and Refs. [61,100–102] to show the calculation of dissipation coefficient for our model. We also refer the reader to see Refs. [69,91,95,99,126,127] for derivation of dissipation coefficient in other warm inflation models.

On accounting for the interactions of the inflaton with intermediate scalar boson χ and fermion ψ_χ, as given in Eqs. (11), (13), the dissipation coefficient at leading order is given as [101]

$$\Upsilon = \frac{2}{T} g^4 \phi^2 \int \frac{d^4p}{(2\pi)^4} [\rho_{\chi_1}(\omega, \boldsymbol{p})^2 + \rho_{\chi_2}(\omega, \boldsymbol{p})^2] \times n_B(\omega)(1 + n_B(\omega)) + \frac{2}{T} g^2 \int \frac{d^4p}{(2\pi)^4} \, tr[\rho_{\psi_\chi}(\omega, \boldsymbol{p})^2] \, n_F(\omega) \, (1 - n_F(\omega)). \tag{A.1}$$

Here $n_B(\omega)$, $n_F(\omega)$ are the Bose–Einstein and Fermi-Dirac distributions, respectively, and ρ_χ, ρ_{ψ_χ} are the spectral functions for the intermediate χ, ψ_χ fields.

$$\begin{aligned} \rho_\chi(\omega, \boldsymbol{p}) &= \frac{i}{p^2 + m^2_{\chi,R} + i\mathrm{Im}\Sigma_\chi} - \frac{i}{p^2 + m^2_{\chi,R} - i\mathrm{Im}\Sigma_\chi} \\ &= \frac{2\ \mathrm{Im}\Sigma_\chi}{(p^2 + m^2_{\chi,R})^2 + (\mathrm{Im}\Sigma_\chi)^2} \\ &= \frac{4\ \omega_p \Gamma_\chi}{(-\omega^2 + \omega_p^2)^2 + 4\ \omega_p^2\ \Gamma_\chi^2}, \end{aligned} \tag{A.2}$$

where Γ_χ is the decay width of the χ field and is related to the imaginary component of the self energy Σ_χ, $\omega_p^2 = |\boldsymbol{p}^2| + m^2_{\chi,R}$ is the dispersion relation of the χ field, and $m^2_{\chi,R} = m^2_\chi + \mathrm{Re}\Sigma_\chi$ is the effective, renormalized mass of the χ field.

The spectral function for fermionic field ψ_χ is given by

$$\rho_{\psi_\chi}(\omega, \boldsymbol{p}) = \frac{i}{\not{p} + m_{\psi_\chi,R} + i\mathrm{Im}\Sigma_{\psi_\chi}} - \frac{i}{\not{p} + m_{\psi_\chi,R} - i\mathrm{Im}\Sigma_{\psi_\chi}}, \tag{A.3}$$

where $m_{\psi_\chi,R} = m_{\psi_\chi} + \mathrm{Re}\Sigma_{\psi_\chi}$ is the effective, renormalized mass, and Σ_{ψ_χ} is the self energy of the ψ_χ field.

Thus, to calculate the dissipation coefficient, we need to compute the masses of χ, ψ_χ fields and their decay width at finite temperature. The decay width of the χ, ψ_χ fields has contributions from direct, inverse as well as thermal scatterings (Landau damping). The response timescale of the system is associated with the decay width as $\tau \rightarrow 1/\Gamma$. For explicit calculations and expressions of the field self energy and decay widths, see Ref. [101].

In certain approximations, the dissipation coefficient given in Eq. (A.1) reduces to simplified expression. In one regime, the poles of the spectral function dominate the integral and is called the pole approximation. In the other regime, the integration is limited to low-momentum and it is referred to as the low-momentum approximation.

A.0.1. Low temperature limit

In this regime, the temperature of the thermal bath is much less than the masses of the intermediate catalyst fields, χ and ψ_χ, i.e. $T \ll m_{\chi,R}, m_{\psi_\chi,R}$, but is higher compared to the radiation fields, $T \gg m_{\sigma,R}, m_{\psi_\sigma,R}$. The thermal corrections to the effective masses of the χ, ψ_χ fields can be neglected in this regime, i.e. $m^2_{\chi,R} \simeq m^2_\chi = 2g^2\varphi^2$ and $m^2_{\psi_\chi,R} \simeq m^2_{\psi_\chi} = 2g^2\varphi^2$. For large values of m_χ/T, the dominant contributions to the dissipation coefficient given in Eq. (A.1) come from virtual χ fields with low energy and momentum, $\omega, |\boldsymbol{p}| \sim T \ll m_\chi$ which leads to the low-momentum approximation. Then, $(\omega^2 - \omega_p^2)^2 \approx m_\chi^4$, and the spectral function for the scalar boson in Eq. (A.2) becomes $\rho_\chi \simeq \frac{4}{m_\chi^3}\Gamma_\chi$, which gives a leading order contribution to the dissipation coefficient, given in Eq. (A.1), $\propto T^3/m_\chi^2$ [100–102]. The fermionic contribution is calculated to be subleading in T in the low temperature limit ($\propto T^5/m^4_{\psi_\chi}$) [100,101].

A detailed analysis including thermal corrections to the χ mass and finite decay width of χ field in the spectral function gives [102]

$$\Upsilon = C_\phi \frac{T^3}{\phi^2}, \tag{A.4}$$

where $C_\phi = \frac{h^2}{16\pi} N_Y N_X$, which depends on the multiplicities of X and Y superfields and coupling between them.

A.0.2. High temperature limit

In this limit, the intermediate catalyst fields are lighter, $m_{\chi,R}$, $m_{\psi_\chi,R} \ll T$. The main contribution to the dissipation coefficient comes from the pole in the spectral function at $\omega = \omega_p$

and a resonant production of on-shell χ particles take place. In the pole approximation, the bosonic spectral function becomes $\rho_\chi^2 \rightarrow \frac{\pi}{2\,\omega_p^2 \Gamma_\chi}\delta(\omega - \omega_p)$. Substituting this in Eq. (A.1) for the scalar field, the dissipation coefficient gets a contribution which is linearly dependent on the temperature of the thermal bath $\Upsilon \approx 0.691\ \frac{g^2}{h^2} T$ [100]. On accounting all the fermionic and bosonic contributions in Eq. (A.1), the total dissipation coefficient is obtained to be [100]

$$\Upsilon = C_T T, \qquad C_T \approx 0.97\ \frac{g^2}{h^2}. \tag{A.5}$$

By knowing the value of C_T, one can calculate the order of ratio of couplings g/h, which is useful in model building.

References

[1] D. Kazanas, Dynamics of the universe and spontaneous symmetry breaking, Astrophys. J. 241 (1980) L59–L63.
[2] K. Sato, First order phase transition of a vacuum and expansion of the universe, Mon. Not. R. Astron. Soc. 195 (1981) 467–479.
[3] A.H. Guth, The inflationary universe: A possible solution to the horizon and flatness problems, Phys. Rev. D23 (1981) 347–356; Adv. Ser. Astrophys. Cosmol. 3 (1987) 139.
[4] A.A. Starobinsky, A new type of isotropic cosmological models without singularity, Phys. Lett. 91B (1980) 99–102, [771(1980)].
[5] A.D. Linde, A new inflationary universe scenario: A possible solution of the horizon, flatness, homogeneity, isotropy and primordial monopole problems, in: Quantum Cosmol., Phys. Lett. 108B (1982) 389–393; Adv. Ser. Astrophys. Cosmol. 3 (1987) 149.
[6] Planck Collaboration, Y. Akrami, et al., Planck 2018 results. X. Constraints on inflation, 2018, arXiv:1807.06211 [astro-ph.CO].
[7] BICEP, Keck Collaboration, P.A.R. Ade, et al., Improved constraints on primordial gravitational waves using Planck, WMAP, and BICEP/Keck observations through the 2018 observing season, Phys. Rev. Lett. 127 (15) (2021) 151301, arXiv:2110.00483 [astro-ph.CO].
[8] D. Baumann, Inflation, in: Physics of the Large and the Small, TASI 09, 1-26 June 2009, 2011, pp. 523–686, arXiv:0907.5424 [hep-th].
[9] A.D. Linde, Inflationary cosmology, Lecture Notes in Phys. 738 (2008) 1–54, arXiv:0705.0164 [hep-th].
[10] S. Tsujikawa, Introductory review of cosmic inflation, in: 2nd Tah Poe School on Cosmology: Modern Cosmology, 2003, arXiv:hep-ph/0304257.
[11] K.A. Olive, Inflation, Phys. Rep. 190 (1990) 307–403.
[12] A. Riotto, Inflation and the theory of cosmological perturbations, ICTP Lect. Notes Ser. 14 (2003) 317–413, arXiv:hep-ph/0210162 [hep-ph].
[13] S. Mollerach, D. Harari, S. Matarrese, CMB polarization from secondary vector and tensor modes, Phys. Rev. D 69 (2004) 063002, arXiv:astro-ph/0310711.
[14] K.N. Ananda, C. Clarkson, D. Wands, The cosmological gravitational wave background from primordial density perturbations, Phys. Rev. D 75 (2007) 123518, arXiv:gr-qc/0612013.
[15] D. Baumann, P.J. Steinhardt, K. Takahashi, K. Ichiki, Gravitational wave spectrum induced by primordial scalar perturbations, Phys. Rev. D 76 (2007) 084019, arXiv:hep-th/0703290.
[16] R. Saito, J. Yokoyama, Gravitational wave background as a probe of the primordial black hole abundance, Phys. Rev. Lett. 102 (2009) 161101, arXiv:0812.4339; Phys. Rev. Lett. 107 (2011) 069901, Erratum.
[17] R. Saito, J. Yokoyama, Gravitational-wave constraints on the abundance of primordial black holes, Progr. Theoret. Phys. 123 (5) (2010) 867–886, arXiv:0912.5317.
[18] S. Wang, Y.-F. Wang, Q.-G. Huang, T.G.F. Li, Constraints on the primordial black hole abundance from the first advanced LIGO observation run using the stochastic gravitational-wave background, Phys. Rev. Lett. 120 (19) (2018) 191102, arXiv:1610.08725 [astro-ph.CO].
[19] S. Clesse, J. García-Bellido, S. Orani, Detecting the stochastic gravitational wave background from primordial black hole formation, 2018, arXiv:1812.11011 [astro-ph.CO].
[20] N. Bartolo, V. De Luca, G. Franciolini, M. Peloso, D. Racco, A. Riotto, Testing primordial black holes as dark matter with LISA, Phys. Rev. D 99 (10) (2019) 103521, arXiv:1810.12224 [astro-ph.CO].
[21] S. Wang, T. Terada, K. Kohri, Prospective constraints on the primordial black hole abundance from the stochastic gravitational-wave backgrounds produced by coalescing events and curvature perturbations, Phys. Rev. D 99 (10) (2019) 103531, arXiv:1903.05924 [astro-ph.CO]; Phys. Rev. D 101 (2020) 069901, Erratum.
[22] J. Kozaczuk, T. Lin, E. Villarama, Signals of primordial black holes at gravitational wave interferometers, Phys. Rev. D 105 (12) (2022) 123023, arXiv:2108.12475 [astro-ph.CO].
[23] Y.B. Zel'dovich, I.D. Novikov, The hypothesis of cores retarded during expansion and the hot cosmological model, Sov. Astron. 10 (1967) 602.
[24] S. Hawking, Gravitationally collapsed objects of very low mass, Mon. Not. R. Astron. Soc. 152 (1971) 75.
[25] B.J. Carr, S.W. Hawking, Black holes in the early universe, Mon. Not. R. Astron. Soc. 168 (1974) 399–415.
[26] B.J. Carr, The primordial black hole mass spectrum, Astrophys. J. 201 (1975) 1–19.
[27] S.W. Hawking, I.G. Moss, J.M. Stewart, Bubble collisions in the very early universe, Phys. Rev. D26 (1982) 2681.
[28] C.J. Hogan, Massive black holes generated by cosmic strings, Phys. Lett. 143B (1984) 87–91.
[29] S.W. Hawking, Black holes from cosmic strings, Phys. Lett. B231 (1989) 237–239.
[30] R.R. Caldwell, A. Chamblin, G.W. Gibbons, Pair creation of black holes by domain walls, Phys. Rev. D53 (1996) 7103–7114, arXiv:hep-th/9602126 [hep-th].
[31] E. Bugaev, P. Klimai, Induced gravitational wave background and primordial black holes, Phys. Rev. D 81 (2) (2010) 023517, arXiv:0908.0664 [astro-ph.CO].
[32] L. Alabidi, K. Kohri, M. Sasaki, Y. Sendouda, Observable spectra of induced gravitational waves from inflation, J. Cosmol. Astropart. Phys. 09 (2012) 017, arXiv:1203.4663 [astro-ph.CO].
[33] K. Inomata, M. Kawasaki, K. Mukaida, T.T. Yanagida, Double inflation as a single origin of primordial black holes for all dark matter and LIGO observations, Phys. Rev. D 97 (4) (2018) 043514, arXiv:1711.06129 [astro-ph.CO].
[34] N. Orlofsky, A. Pierce, J.D. Wells, Inflationary theory and pulsar timing investigations of primordial black holes and gravitational waves, Phys. Rev. D 95 (6) (2017) 063518, arXiv:1612.05279 [astro-ph.CO].
[35] W. Ahmed, M. Junaid, U. Zubair, Primordial black holes and gravitational waves in hybrid inflation with chaotic potentials, 2021, arXiv:2109.14838 [astro-ph.CO].
[36] C. Fu, P. Wu, H. Yu, Scalar induced gravitational waves in inflation with gravitationally enhanced friction, Phys. Rev. D 101 (2) (2020) 023529, arXiv:1912.05927 [astro-ph.CO].
[37] Q. Gao, Primordial black holes and secondary gravitational waves from chaotic inflation, Sci. China Phys. Mech. Astron. 64 (8) (2021) 280411, arXiv:2102.07369 [gr-qc].
[38] Z. Yi, Q. Gao, Y. Gong, Z.-h. Zhu, Primordial black holes and scalar-induced secondary gravitational waves from inflationary models with a noncanonical kinetic term, Phys. Rev. D 103 (6) (2021) 063534, arXiv:2011.10606 [astro-ph.CO].
[39] J. Lin, S. Gao, Y. Gong, Y. Lu, Z. Wang, F. Zhang, Primordial black holes and scalar induced secondary gravitational waves from Higgs inflation with non-canonical kinetic term, 2021, arXiv:2111.01362 [gr-qc].
[40] S. Kawai, J. Kim, Primordial black holes from Gauss-Bonnet-corrected single field inflation, Phys. Rev. D 104 (8) (2021) 083545, arXiv:2108.01340 [astro-ph.CO].
[41] N. Bhaumik, R.K. Jain, Small scale induced gravitational waves from primordial black holes, a stringent lower mass bound, and the imprints of an early matter to radiation transition, Phys. Rev. D 104 (2) (2021) 023531, arXiv:2009.10424 [astro-ph.CO].
[42] H.V. Ragavendra, P. Saha, L. Sriramkumar, J. Silk, Primordial black holes and secondary gravitational waves from ultraslow roll and punctuated inflation, Phys. Rev. D 103 (8) (2021) 083510, arXiv:2008.12202 [astro-ph.CO].
[43] J. Lin, Q. Gao, Y. Gong, Y. Lu, C. Zhang, F. Zhang, Primordial black holes and secondary gravitational waves from k and G inflation, Phys. Rev. D 101 (10) (2020) 103515, arXiv:2001.05909 [gr-qc].
[44] B.P. Abbott, et al., An upper limit on the stochastic gravitational-wave background of cosmological origin, Nature 460 (7258) (2009) 990–994, arXiv:0910.5772 [astro-ph.CO].
[45] H. Assadullahi, D. Wands, Constraints on primordial density perturbations from induced gravitational waves, Phys. Rev. D 81 (2010) 023527, arXiv:0907.4073 [astro-ph.CO].
[46] K. Inomata, T. Nakama, Gravitational waves induced by scalar perturbations as probes of the small-scale primordial spectrum, Phys. Rev. D 99 (4) (2019) 043511, arXiv:1812.00674 [astro-ph.CO].
[47] L. Lentati, et al., European pulsar timing array limits on an isotropic stochastic gravitational-wave background, Mon. Not. R. Astron. Soc. 453 (3) (2015) 2576–2598, arXiv:1504.03692 [astro-ph.CO].
[48] NANOGrav Collaboration, Z. Arzoumanian, et al., The nanograv nine-year data set: Limits on the isotropic stochastic gravitational wave background, Astrophys. J. 821 (1) (2016) 13, arXiv:1508.03024 [astro-ph.GA].
[49] G. Janssen, et al., Gravitational wave astronomy with the SKA, in: T.L. Bourke, et al. (Eds.), PoS AASKA14 (2015) 037, arXiv:1501.00127 [astro-ph.IM].

[50] KAGRA, LIGO Scientific, Virgo, VIRGO Collaboration, B.P. Abbott, et al., Prospects for observing and localizing gravitational-wave transients with advanced LIGO, advanced Virgo and KAGRA, Living Rev. Rel. 21 (1) (2018) 3, arXiv:1304.0670 [gr-qc].

[51] P. Amaro-Seoane, et al., Laser interferometer space antenna, 2017, arXiv e-prints, arXiv:1702.00786 [astro-ph.IM].

[52] K. Yagi, N. Seto, Detector configuration of DECIGO/BBO and identification of cosmological neutron-star binaries, Phys. Rev. D 83 (2011) 044011, arXiv:1101.3940 [astro-ph.CO]; Phys. Rev. D 95 (2017) 109901, Erratum.

[53] Einstein Telescope webpage, http://www.et-gw.eu/.

[54] S. Dwyer, D. Sigg, S.W. Ballmer, L. Barsotti, N. Mavalvala, M. Evans, Gravitational wave detector with cosmological reach, Phys. Rev. D 91 (8) (2015) 082001, arXiv:1410.0612 [astro-ph.IM].

[55] G. Domènech, Scalar induced gravitational waves review, Universe 7 (11) (2021) 398, arXiv:2109.01398 [gr-qc].

[56] L. Bian, et al., The gravitational-wave physics II: Progress, Sci. China Phys. Mech. Astron. 64 (12) (2021) 120401, arXiv:2106.10235 [gr-qc].

[57] A. Berera, L.-Z. Fang, Thermally induced density perturbations in the inflation era, Phys. Rev. Lett. 74 (1995) 1912–1915, arXiv:astro-ph/9501024 [astro-ph].

[58] A. Berera, Warm inflation, Phys. Rev. Lett. 75 (1995) 3218–3221, arXiv:astro-ph/9509049 [astro-ph].

[59] A. Berera, M. Gleiser, R.O. Ramos, A first principles warm inflation model that solves the cosmological horizon / flatness problems, Phys. Rev. Lett. 83 (1999) 264–267, arXiv:hep-ph/9809583 [hep-ph].

[60] A. Berera, The warm inflationary universe, Contemp. Phys. 47 (2006) 33–49, arXiv:0809.4198 [hep-ph].

[61] A. Berera, I.G. Moss, R.O. Ramos, Warm inflation and its microphysical basis, Rep. Progr. Phys. 72 (2009) 026901, arXiv:0808.1855 [hep-ph].

[62] M. Bastero-Gil, A. Berera, N. Kronberg, Exploring the parameter space of warm-inflation models, J. Cosmol. Astropart. Phys. 1512 (12) (2015) 046, arXiv:1509.07604 [hep-ph].

[63] L. Visinelli, Observational constraints on monomial warm inflation, J. Cosmol. Astropart. Phys. 1607 (07) (2016) 054, arXiv:1605.06449 [astro-ph.CO].

[64] M. Benetti, R.O. Ramos, Warm inflation dissipative effects: Predictions and constraints from the Planck data, Phys. Rev. D95 (2) (2017) 023517, arXiv:1610.08758 [astro-ph.CO].

[65] R. Arya, A. Dasgupta, G. Goswami, J. Prasad, R. Rangarajan, Revisiting CMB constraints on warm inflation, J. Cosmol. Astropart. Phys. 1802 (02) (2018) 043, arXiv:1710.11109 [astro-ph.CO].

[66] M. Bastero-Gil, S. Bhattacharya, K. Dutta, M.R. Gangopadhyay, Constraining warm inflation with CMB data, J. Cosmol. Astropart. Phys. 1802 (02) (2018) 054, arXiv:1710.10008 [astro-ph.CO].

[67] R. Arya, R. Rangarajan, Study of warm inflationary models and their parameter estimation from CMB, 2018, arXiv:1812.03107 [astro-ph.CO].

[68] R. Arya, Formation of primordial black holes from warm inflation, J. Cosmol. Astropart. Phys. 09 (2020) 042, arXiv:1910.05238 [astro-ph.CO].

[69] M. Bastero-Gil, M.S. Díaz-Blanco, Gravity waves and primordial black holes in scalar warm little inflation, J. Cosmol. Astropart. Phys. 12 (12) (2021) 052, arXiv:2105.08045 [hep-ph].

[70] N. Aggarwal, et al., Searching for new physics with a levitated-sensor-based gravitational-wave detector, Phys. Rev. Lett. 128 (11) (2022) 111101, arXiv:2010.13157 [gr-qc].

[71] P. Bernard, A. Chincarini, G. Gemme, R. Parodi, E. Picasso, A detector of gravitational waves based on coupled microwave cavities, 2002, arXiv:gr-qc/0203024.

[72] Holometer Collaboration, A.S. Chou, et al., MHz gravitational wave constraints with decameter Michelson interferometers, Phys. Rev. D 95 (6) (2017) 063002, arXiv:1611.05560 [astro-ph.IM].

[73] O.D. Aguiar, The past, present and future of the resonant-mass gravitational wave detectors, Res. Astron. Astrophys. 11 (2011) 1–42, arXiv:1009.1138 [astro-ph.IM].

[74] A. Berera, Interpolating the stage of exponential expansion in the early universe: A possible alternative with no reheating, Phys. Rev. D 55 (1997) 3346–3357, arXiv:hep-ph/9612239.

[75] S. Gupta, A. Berera, A.F. Heavens, S. Matarrese, Non-Gaussian signatures in the cosmic background radiation from warm inflation, Phys. Rev. D66 (2002) 043510, arXiv:astro-ph/0205152 [astro-ph].

[76] I.G. Moss, T. Yeomans, Non-gaussianity in the strong regime of warm inflation, J. Cosmol. Astropart. Phys. 1108 (2011) 009, arXiv:1102.2833 [astro-ph.CO].

[77] A. Berera, Warm inflation solution to the eta problem, in: Proceedings, International Workshop on Astroparticle and High-Energy Physics, AHEP-2003: Valencia, Spain, October 14-18, 2003, 2004, AHEP2003/069, arXiv:hep-ph/0401139 [hep-ph]. PoSAHEP 2003 (2003) 069.

[78] J.G. Rosa, L.B. Ventura, Warm little inflaton becomes cold dark matter, Phys. Rev. Lett. 122 (16) (2019) 161301, arXiv:1811.05493 [hep-ph].

[79] J.G. Rosa, L.B. Ventura, Warm little inflaton becomes dark energy, Phys. Lett. B 798 (2019) 134984, arXiv:1906.11835 [hep-ph].

[80] P.M. Sá, Triple unification of inflation, dark energy, and dark matter in two-scalar-field cosmology, Phys. Rev. D 102 (10) (2020) 103519, arXiv:2007.07109 [gr-qc].

[81] R. D'Agostino, O. Luongo, Cosmological viability of a double field unified model from warm inflation, Phys. Lett. B 829 (2022) 137070, arXiv:2112.12816 [astro-ph.CO].

[82] M.R. Gangopadhyay, S. Myrzakul, M. Sami, M.K. Sharma, Paradigm of warm quintessential inflation and production of relic gravity waves, Phys. Rev. D 103 (4) (2021) 043505, arXiv:2011.09155 [astro-ph.CO].

[83] M. Bastero-Gil, A. Berera, R.O. Ramos, J.G. Rosa, Warm baryogenesis, Phys. Lett. B 712 (2012) 425–429, arXiv:1110.3971 [hep-ph].

[84] S. Basak, S. Bhattacharya, M.R. Gangopadhyay, N. Jaman, R. Rangarajan, M. Sami, The paradigm of warm quintessential inflation and spontaneous baryogenesis, J. Cosmol. Astropart. Phys. 03 (03) (2022) 063, arXiv:2110.00607 [astro-ph.CO].

[85] S. Das, Warm inflation in the light of swampland criteria, Phys. Rev. D99 (6) (2019) 063514, arXiv:1810.05038 [hep-th].

[86] M. Motaharfar, V. Kamali, R.O. Ramos, Warm inflation as a way out of the Swampland, Phys. Rev. D99 (6) (2019) 063513, arXiv:1810.02816 [astro-ph.CO].

[87] E. Calzetta, B.L. Hu, Nonequilibrium quantum fields: Closed-time-path effective action, wigner function, and Boltzmann equation, Phys. Rev. D 37 (1988) 2878–2900, URL https://link.aps.org/doi/10.1103/PhysRevD.37.2878.

[88] M. Gleiser, R.O. Ramos, Microphysical approach to nonequilibrium dynamics of quantum fields, Phys. Rev. D50 (1994) 2441–2455, arXiv:hep-ph/9311278 [hep-ph].

[89] A.K. Das, Finite Temperature Field Theory, World Scientific, New York, 1997.

[90] M. Le Bellac, Thermal Field Theory, in: Cambridge Monographs on Mathematical Physics, Cambridge University Press, 1996.

[91] A. Berera, M. Gleiser, R.O. Ramos, Strong dissipative behavior in quantum field theory, Phys. Rev. D 58 (1998) 123508, arXiv:hep-ph/9803394.

[92] L.M.H. Hall, I.G. Moss, A. Berera, Scalar perturbation spectra from warm inflation, Phys. Rev. D69 (2004) 083525, arXiv:astro-ph/0305015 [astro-ph].

[93] I.G. Moss, C. Xiong, On the consistency of warm inflation, J. Cosmol. Astropart. Phys. 0811 (2008) 023, arXiv:0808.0261 [astro-ph].

[94] J. Yokoyama, A.D. Linde, Is warm inflation possible? Phys. Rev. D 60 (1999) 083509, arXiv:hep-ph/9809409.

[95] M. Bastero-Gil, A. Berera, R. Hernández-Jiménez, J.G. Rosa, Warm inflation within a supersymmetric distributed mass model, Phys. Rev. D99 (10) (2019) 103520, arXiv:1812.07296 [hep-ph].

[96] A. Berera, R.O. Ramos, The affinity for scalar fields to dissipate, Phys. Rev. D63 (2001) 103509, arXiv:hep-ph/0101049 [hep-ph].

[97] A. Berera, R.O. Ramos, Dynamics of interacting scalar fields in expanding space-time, Phys. Rev. D71 (2005) 023513, arXiv:hep-ph/0406339 [hep-ph].

[98] M. Bastero-Gil, A. Berera, R.O. Ramos, J.G. Rosa, Warm little inflaton, Phys. Rev. Lett. 117 (15) (2016) 151301, arXiv:1604.08838 [hep-ph].

[99] M. Bastero-Gil, A. Berera, R.O. Ramos, J.G. Rosa, Towards a reliable effective field theory of inflation, Phys. Lett. B 813 (2021) 136055.

[100] I.G. Moss, C. Xiong, Dissipation coefficients for supersymmetric inflatonary models, 2006, arXiv:hep-ph/0603266 [hep-ph].

[101] M. Bastero-Gil, A. Berera, R.O. Ramos, Dissipation coefficients from scalar and fermion quantum field interactions, J. Cosmol. Astropart. Phys. 1109 (2011) 033, arXiv:1008.1929 [hep-ph].

[102] M. Bastero-Gil, A. Berera, R.O. Ramos, J.G. Rosa, General dissipation coefficient in low-temperature warm inflation, J. Cosmol. Astropart. Phys. 1301 (2013) 016, arXiv:1207.0445 [hep-ph].

[103] C. Graham, I.G. Moss, Density fluctuations from warm inflation, J. Cosmol. Astropart. Phys. 0907 (2009) 013, arXiv:0905.3500 [astro-ph.CO].

[104] M. Bastero-Gil, A. Berera, R.O. Ramos, Shear viscous effects on the primordial power spectrum from warm inflation, J. Cosmol. Astropart. Phys. 1107 (2011) 030, arXiv:1106.0701 [astro-ph.CO].

[105] R.O. Ramos, L.A. da Silva, Power spectrum for inflation models with quantum and thermal noises, J. Cosmol. Astropart. Phys. 1303 (2013) 032, arXiv:1302.3544 [astro-ph.CO].

[106] S. Bartrum, M. Bastero-Gil, A. Berera, R. Cerezo, R.O. Ramos, J.G. Rosa, The importance of being warm (during inflation), Phys. Lett. B732 (2014) 116–121, arXiv:1307.5868 [hep-ph].

[107] J.R. Espinosa, D. Racco, A. Riotto, A cosmological signature of the SM higgs instability: Gravitational waves, J. Cosmol. Astropart. Phys. 09 (2018) 012, arXiv:1804.07732 [hep-ph].

[108] K. Kohri, T. Terada, Semianalytic calculation of gravitational wave spectrum nonlinearly induced from primordial curvature perturbations, Phys. Rev. D 97 (12) (2018) 123532, arXiv:1804.08577 [gr-qc].

[109] M. Maggiore, Gravitational wave experiments and early universe cosmology, Phys. Rep. 331 (2000) 283–367, arXiv:gr-qc/9909001.

[110] C.J. Moore, R.H. Cole, C.P.L. Berry, Gravitational-wave sensitivity curves, Classical Quantum Gravity 32 (1) (2015) 015014, arXiv:1408.0740 [gr-qc].
[111] V. Mandic, E. Floden, GW plotter webpage, https://homepages.spa.umn.edu/gwplotter.
[112] LIGO Scientific Collaboration, B. Abbott, et al., Searching for a stochastic background of gravitational waves with LIGO, Astrophys. J. 659 (2007) 918–930, arXiv:astro-ph/0608606.
[113] I. Sendra, T.L. Smith, Improved limits on short-wavelength gravitational waves from the cosmic microwave background, Phys. Rev. D 85 (2012) 123002, arXiv:1203.4232 [astro-ph.CO].
[114] T.L. Smith, E. Pierpaoli, M. Kamionkowski, A new cosmic microwave background constraint to primordial gravitational waves, Phys. Rev. Lett. 97 (2006) 021301, arXiv:astro-ph/0603144.
[115] L. Pagano, L. Salvati, A. Melchiorri, New constraints on primordial gravitational waves from Planck 2015, Phys. Lett. B 760 (2016) 823–825, arXiv:1508.02393 [astro-ph.CO].
[116] M. Parikh, F. Wilczek, G. Zahariade, Signatures of the quantization of gravity at gravitational wave detectors, Phys. Rev. D 104 (4) (2021) 046021, arXiv:2010.08208 [hep-th].
[117] V. Mandic, E. Floden, LIGO Document Control Center Portal, https://dcc.ligo.org/login/index.shtml?entityID=https%3A%2F%2Fdcc.ligo.org%2Fshibboleth-sp&return=https%3A%2F%2Fdcc.ligo.org%2FShibboleth.sso%2FLogin%3FSAMLDS%3D1%26target%3Dss%253Amem%253Ab56ec8609becaa7774c5954273c049e9eebdb089.
[118] C.J. Hogan, P.L. Bender, Estimating stochastic gravitational wave backgrounds with sagnac calibration, Phys. Rev. D 64 (2001) 062002, arXiv:astro-ph/0104266.
[119] N.J. Cornish, Detecting a stochastic gravitational wave background with the laser interferometer space antenna, Phys. Rev. D 65 (2002) 022004, arXiv:gr-qc/0106058.
[120] V. Corbin, N.J. Cornish, Detecting the cosmic gravitational wave background with the big bang observer, Classical Quantum Gravity 23 (2006) 2435–2446, arXiv:gr-qc/0512039.
[121] S. Sato, et al., The status of DECIGO, in: D. Giardini, P. Jetzer (Eds.), J. Phys. Conf. Ser. 840 (1) (2017) 012010.
[122] F.A. Jenet, et al., Upper bounds on the low-frequency stochastic gravitational wave background from pulsar timing observations: Current limits and future prospects, Astrophys. J. 653 (2006) 1571–1576, arXiv:astro-ph/0609013.
[123] N. Aggarwal, et al., Challenges and opportunities of gravitational-wave searches at MHz to GHz frequencies, Living Rev. Rel. 24 (1) (2021) 4, arXiv:2011.12414 [gr-qc].
[124] A. Berlin, et al., Detecting high-frequency gravitational waves with microwave cavities, 2021, arXiv:2112.11465 [hep-ph].
[125] L. notes on Non-equilibrium Quantum Field Theory and cosmological applications, http://gravitation.web.ua.pt/jrosa.
[126] S. Das, R.O. Ramos, Runaway potentials in warm inflation satisfying the Swampland conjectures, Phys. Rev. D 102 (10) (2020) 103522, arXiv:2007.15268 [hep-th].
[127] S. Material, http://link.aps.org/supplemental/10.1103/PhysRevLett.122.161301.